crystals

MDPI

Article

Study on Scale and Corrosion Inhibition Performance of Phosphorus-Free Copolymer Hydroxyethyl Methacrylate-Acrylic Acid-Sodium Allyl Sulfonate

Rong Yu, Huan Lei * and Zhao Tian

College of Urban Planning and Municipal Engineering, Xi'an Polytechnic University, Xi'an 710048, China
* Correspondence: 201421022@stu.xpu.edu.cn

Abstract: A free radical polymerization method was used to synthesize the phosphorus-free copolymer hydroxyethyl methacrylate-acrylic acid-sodium allyl sulfonate (HEMA-AA-SAS). The structure of HEMA-AA-SAS was characterized, and the scale inhibition performance of the copolymer was determined. Near 100% of scale inhibition was achieved when the copolymer concentration was 6 mg/L, suggesting that HEMA-AA-SAS had a significant effect on the inhibition efficiency. The corrosion inhibition performance of the copolymer and the effects under different water quality conditions were determined using a rotating sample method. When the copolymer with 7.5 mg/L was implemented, the corrosion inhibition effect on the carbon steel hanging sheet reached 88.12%. The effects of copolymers on calcium carbonate crystals were analyzed using scanning electron microscopy (SEM) and X-ray powder diffraction (XRD), which showed that the copolymers could destroy crystal morphology effectively. Through the calculation of the corrosion activation energy, the results show that the corrosion activation energy increases and the corrosion reaction rate decreases after the copolymer has been added. The copolymer HEMA-AA-SAS has excellent scale and corrosion inhibition performance.

Keywords: phosphorus-free copolymer; scale inhibitor performance; corrosion inhibition performance; decentralized performance; corrosion activation energy

check for updates

Citation: Yu, R.; Lei, H.; Tian, Z. Study on Scale and Corrosion Inhibition Performance of Phosphorus-Free Copolymer Hydroxyethyl Methacrylate-Acrylic Acid-Sodium Allyl Sulfonate. *Crystals* **2023**, *13*, 418. https://doi.org/10.3390/cryst13030418

Academic Editors: Jesús Sanmartín-Matalobos and George D. Verros

Received: 13 January 2023
Revised: 19 February 2023
Accepted: 20 February 2023
Published: 28 February 2023

1. Introduction

Industrial production uses demineralized water, desalinated water, and circulating cooling water in large quantities [1–3]. In the working process of these systems, scaling and corrosion problems often occur, which affect the life and normal operation of pipelines and equipment and cause huge economic losses. The most economical and effective way is to add scale and corrosion inhibitor [4–8]. It can increase the solubility product of calcium carbonate and other salts and ensure the safe operation of the water system [9].

Phosphorus-based agents have the characteristics of low doses and high efficiency, but phosphorus-containing scale inhibitor can bring nutrients to plants causing eutrophication of water bodies and damage to the environment. Therefore, the development of phosphorus-free, environmentally friendly agents is the trend in scale inhibitors [10–12]. The novel copolymer scale and corrosion inhibitors have the characteristics of high efficiency and multi-function without polluting the environment and have become a hot spot of current research [13–15].

The scale inhibition effect of copolymers is burdened by the active groups in the molecule, including carboxyl, hydroxyl, sulfonic acid, ester groups, etc. Weakly acidic or weakly hydrophilic groups such as carboxyl and hydroxyl have a good inhibition effect on calcium carbonate and calcium sulfate, but when the concentration of the group is too high, it is easy to form calcium gel with calcium ions, and hydroxyl and sulfonic acid groups have a good inhibition effect on calcium phosphate. Sulfonic acid and ester groups can

prevent the weak acid calcium gel generation, with adsorption, and can disperse metal oxides and stabilize zinc.

Acrylic acid is a colorless liquid with a strong acidity, a strong irritating odor, and miscible with water; its molecular structure contains double bonds and carboxyl groups, which can easily undergo addition reactions, and the carboxyl group in the molecule can effectively curb calcium carbonate scaling. Hydroxyethyl methacrylate, colorless and transparent, contains polymerizable vinyl, ester group, and active hydroxyl group; its polymer has hydrophilic and pro-metal ion characteristics. Sodium allyl sulfonate, a white solid with double bonds and sulfonic acid groups, does not contain nitrogen, phosphorus, or benzene ring; copolymerization with acrylic acid has a good effect on blocking calcium carbonate, calcium phosphate scale, etc. In this paper, a new non-phosphorus, environmentally friendly copolymer scale inhibitor (HEMA-AA-SAS) was synthesized by free-radical polymerization. The molecular structure of the scale inhibitor determines its performance. The synergistic effect between the active groups improves the scale inhibition, dispersion, and corrosion inhibition effect of the copolymer [16,17]. The scale inhibition, dispersion, and corrosion inhibition performance were analyzed. The properties and the principle of copolymers' function were studied.

2. Materials and Method

2.1. Chemicals

The reagents are acrylic acid (Xi'an, China, analytical purity, Xi'an Chemical Reagent Factory); hydroxyethyl methacrylate, sodium allyl sulfonate (Shanghai, China, both analytical purity, Shanghai Maclean Biochemical Technology Co., Ltd.); calcium chloride (Tianjin, China, analytical purity, Jiaxing Changli Chemical Co., Ltd.); sodium bicarbonate (Tianjin, China, analytical purity, Tianjin Chemical Reagent Factory); ethylenediaminetetraacetic acid (Tianjin, China, analytical purity, Tianjin Comio Chemical Reagent Co., Ltd.); sodium hydroxide; hydrochloric acid (Shanghai, China, analytical purity, Shanghai Huichuang Chemical Reagent Factory).

The instruments used were HHS-21-8 electric thermostatic water bath (Shanghai, China, HHS-21-8, Shanghai Boxun Industry Co., Ltd.); Siemens RCC-I rotary coupon corrosion tester (Jiangsu, China, RCC-I, Motian Electronic Instruments Co., Ltd.); AL204 electronic balance (Jiangsu, China, AL204, Jintan Ruihua Co., Ltd.); Wika UPT-II-20 T benchtop ultra-pure water machine (Chengdu, China, UPT-II-20T, Chengdu Ultra Pure Technology Co., Ltd.); far infrared rapid drying oven (Shanghai, China, DZF-6030, Shanghai Jinghong Experimental Equipment Co., Ltd.); Hitachi S-4800 scanning electron microscope (Tokyo, Japan, S-4800, Hitachi, Japan); Nicolet 5700 type infrared spectrometer (Hangzhou, China, Nicolet 5700, Hangzhou Hanze Instrument Co.)

2.2. Reaction Set-Up

The copolymer HEMA-AA-SAS was synthesized using free radical polymerization of an aqueous solution. A three-port flask with a constant pressure drop funnel and a reflux condensing tube was placed in a water bath containing a magnetic stirrer and a thermometer. The concentrations of hydroxyethyl methacrylate, acrylic acid, sodium allyl sulfonate (total mass of copolymer is 6 g, configured in molar ratios of HEMA:AA:SAS = 1:6:1, 1:8:1, 1:10:1), and tert-butanol were added to a three-necked flask with a magnetic stirrer turned on and the temperature set at 80 °C. A certain concentration of ammonium persulfate was added into a constant pressure funnel, and controlling its dropping speed, keeping the temperature for a certain time after dropping, making the solution uniformly react completely. Naturally cooling to room temperature, a pale yellow transparent liquid can be obtained; adding potassium hydroxide solution to the copolymer to adjust pH to 5.0, after anhydrous ethanol precipitation, the yellow viscous liquid at the bottom of the solution was dried at 50 °C after vacuum extraction and filtration, then the purified copolymer corrosion and scale inhibitor was obtained. The synthesis process is shown in Figure 1.

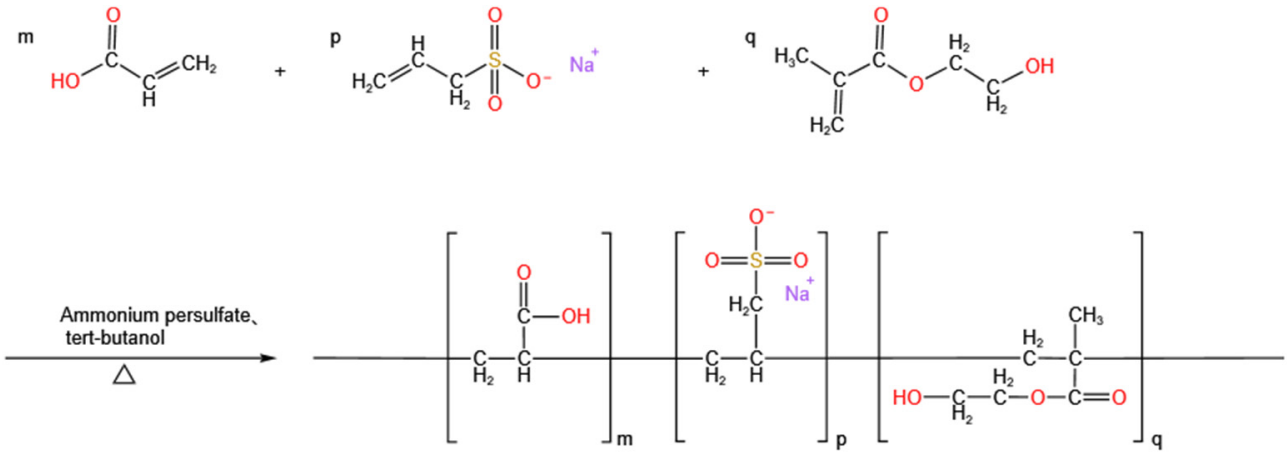

Figure 1. Synthesis process of HEMA-AA-SAS.

2.3. Scale Inhibition Performance

The scale inhibition performance of the copolymer on calcium carbonate was determined using the static scale inhibition method [10]. A calcium ion solution of 200 mg/L and carbonate solution of 500 mg/L were added to the conical flask. Different concentrations of copolymer scale inhibitors were added. The pH of the solution, after setting the water bath time and testing the water sample after the reaction was cooled and filtered, was varied. Using EDTA standard titration, the scale inhibition rate was calculated.

Scanning electron microscopy (SEM) was used to observe the morphology changes in the crystals before and after the addition of the copolymers. Also, a sample was dried, ground, and measured by XRD to determine the phases.

2.4. Dispersion Performance

Different solutions were prepared: $CaCl_2$ solutions, $FeSO_4 \cdot 7H_2O$ solutions, and copolymer scale inhibitor solutions with different concentrations, so that $C[Ca^{2+}]$ = 200 mg/L, $C[Fe^{2+}]$ = 20 mg/L. The concentration of sodium tetraborate was 15.2 g/L to adjust pH to 9, at a constant temperature water bath at 80 °C for 5 h. Solutions were filtered after cooling, and the supernatant was taken and the light transmittance of the solution was measured with a spectrophotometer at 420 nm.

Then, a 0.1% kaolin solution was prepared, adding certain concentrations of Ca^{2+} and $CO_3{}^{2-}$ solutions and copolymer solutions of different concentrations. They were well and then bathed at a constant temperature of 80 °C for 5 h. After cooling, the solution was filtered to measure the turbidity of the solution at 420 nm. The higher the turbidity of the solution, the better the dispersion silicon effect of the copolymer.

2.5. Corrosion Inhibition Performance

The corrosion inhibition effect of copolymers on metals was determined using the rotating hanging tablet method. A3 (I) carbon steel was selected for the specimen. The speed of the hanging tablet was 75 r/min, and the experimental time was set to 72 h. For calculating corrosion rate and inhibition rate, see Equations (1) and (2):

$$v = \frac{8760(m - m_0) \times 10}{s\rho t} \tag{1}$$

where v is corrosion rate, m m/a; m is mass loss value of test piece, g; m_0 is mass loss value of test piece in blank experiment, g; s is surface area of test piece, cm^2; ρ is density of test piece, g/cm^3; t is test time, h.

$$\eta = \frac{v_0 - v_1}{v_0} \times 100\% \tag{2}$$

with v_0 the corrosion rate of blank test and v_1 the corrosion rate of the test piece (in mm/a).

3. Results and Discussions

3.1. Structure Characterization of HEMA-AA-SAS

In the range of 4000–500 cm^{-1} wavelengths, the copolymers synthesized under different ratios were analyzed using FT-IR.

Figure 2 is the infrared spectrum of the copolymer synthesized using monomers with different ratios. The FTIR spectrum shows the following absorption bands: 599.1 cm^{-1} (-C-S stretching vibration absorption peak); 1401 and 1044.5 cm^{-1} (both peaks belong to sulfonic acid group); 1191.5 cm^{-1} (-C=O symmetric stretching vibration absorption peak); 1727.9 cm^{-1} (-C=O stretching vibration absorption peak); 3443.0 cm^{-1} (the peak belongs to the hydroxyl group). It shows that the copolymer corrosion and scale inhibitor contains a large number of carboxyl groups, and the scale inhibition effect on calcium carbonate is better. It shows that the copolymer corrosion and scale inhibitor contains hydroxyl groups. Based on the above analysis, it shows that the copolymer corrosion and scale inhibitor synthesized under optimized conditions meets the design concept.

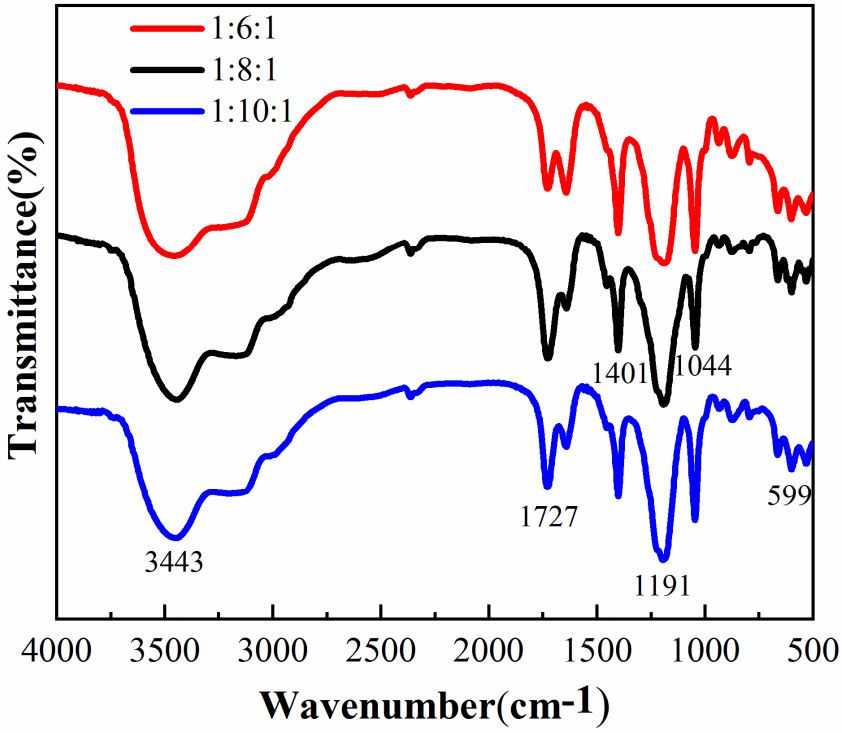

Figure 2. Infrared spectrum of HEMA−AA−SAS.

The copolymer scale inhibitor contains functional groups such as carboxyl group, sulfonic group, hydroxyl group, and ester group. After hydrolysis of the scale inhibitor, the molecular chain forms a water-soluble complex with the scaling cation in water, thus reducing the formation of scale particles; in the process of scale inhibition, the molecular chains adsorb many crystallites with the same charge. The collision accumulation between the crystallites is reduced due to the electrostatic repulsion, and the functional groups in the molecules are adsorbed on the growing points of inorganic salt crystals so that the crystals cannot grow properly and that they are distorted.

3.2. Scale Inhibition of HEMA-AA-SAS

3.2.1. Effect of Different Dosage on Scale Inhibition Performance of Copolymer

As shown in Figure 3, the scale inhibition rate increases with the increase in HEMA-AA-SAS concentration. Polyaspartic acid (PASP), (PAA), and polyepoxysuccinic acid (PESA) are industrially pure, supplied by the Shandong Province Taihe Water Treatment Co. The scale inhibition rate reaches 99% when the concentration of the scale inhibitor

is 6 mg/L. After that, the scale inhibitor decreases with the increase in scale inhibitor concentration, but the scale inhibition effect is still above 90%. When the concentration of the scale inhibitor increases, the content of the functional groups gradually increases, and the scale inhibition effect also steadily increases. However, when the concentration of the scale inhibitor is too high, the functional groups in the molecule agglomerate due to polarity effects [18]. Moreover, the hydrogen bond formed between the functional groups and the oxygen atoms on the surface of the crystal increase the repulsive force by increasing the charge. When the concentration is too high, the repulsion between the crystals will be weakened, and the scale inhibition effect will not continue to increase, indicating that there is a threshold effect of the scale inhibitor [19]. Compared with other commercially available scale inhibitors, HEMA-AA-SAS has the best scale inhibition effect at the same concentration. The reason is that the functional group contained in the copolymer molecule complexes with calcium ions to form a water-soluble compound [20].

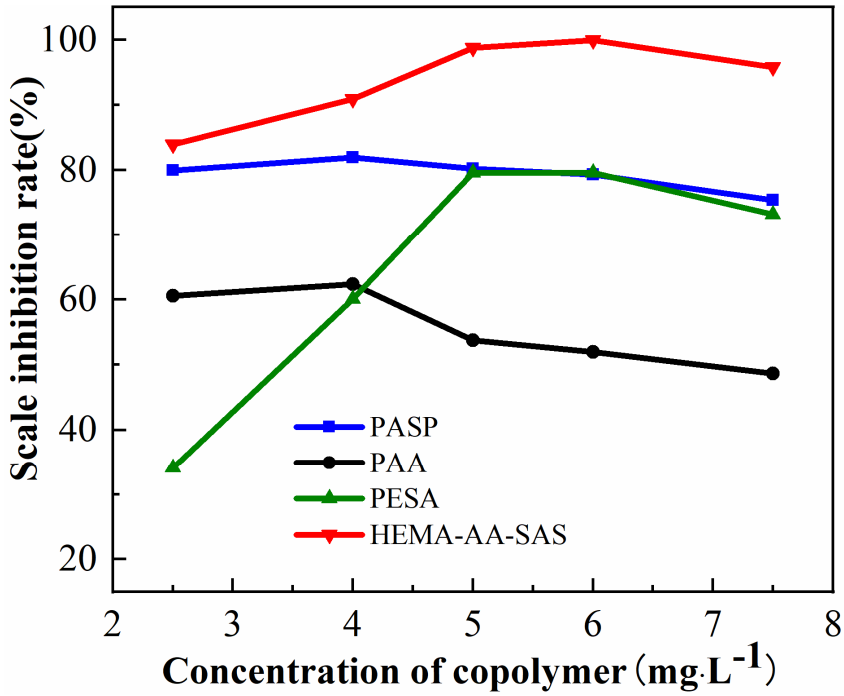

Figure 3. Influence of copolymer dosage on scale inhibition performance.

3.2.2. Effect of Different Ca^{2+} Concentrations on Scale Inhibition Performance of Copolymer: Effect of the Calcium Ion and Copolymer Concentrations on Scale Inhibition at a pH of 8.0

Figure 4 shows that when the copolymer dosage is at low concentration, it has a better scale inhibition effect on $CaCO_3$ scale. The functional group such as a carboxyl group contained in the solution forms a chelate compound soluble in water with Ca^{2+} to reduce the formation of calcium scale. With an increase in the concentration of scale inhibitor, the scale inhibition effect of water samples with different calcium ion concentration mainly increased at first and then decreased. Compared with the water samples of higher calcium ion concentration, when the water samples with lower calcium ion concentration achieve the optimal scale inhibition effect, the continuous increase in the dosage of the copolymer is less affected. When the calcium ion concentration exceeds 600 mg/L, the scale inhibitor concentration exceeds 5 mg/L. As the calcium content in the water sample increases, the formation of calcium carbonate is promoted, and a polarity effect is likely to occur when the concentration of the scale inhibitor is large. The repulsion between the calcium carbonate grains is weakened, so that the scale inhibition rate will be greatly reduced.

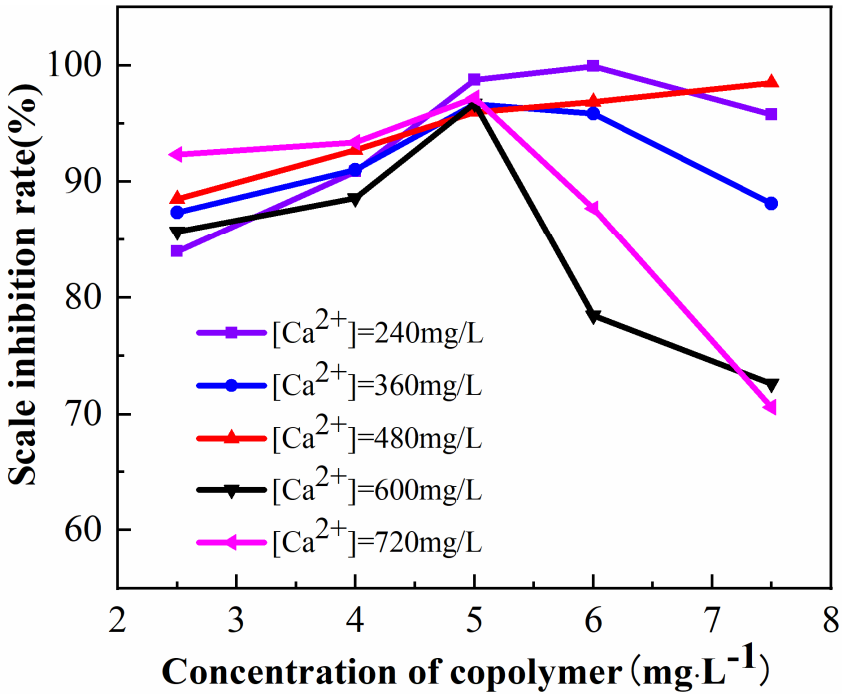

Figure 4. Influence of Ca^{2+} dosage on scale inhibition performance.

3.3. Dispersion Properties of HEMA-AA-SAS

3.3.1. Effect of Copolymer Concentration on Properties of Dispersed Iron

Prepare a certain concentration of $CaCl_2$ solution, $FeSO_4$-$7H_2O$ solution, and copolymer scale inhibitor solution containing different dosing amounts, so that C[Ca^{2+}] = 200 mg/L, C[Fe^{2+}] = 20 mg/L; adjust the pH to 9 using a concentration of 15.2 g/L sodium tetraborate, at a temperature of 80 °C; keep constant temperature water bath for 5 h, then cool to room temperature. After the experiment, the specimen solution filtration was performed, the filtrate was removed, and the transmittance of the solution was measured at 420 nm by spectrophotometer.

The other reaction conditions were controlled constant, and the amount of scale inhibitor was changed to determine the dispersion effect of four scale inhibitors on iron oxide at different concentrations; the results are shown in Figure 4.

Fe^{2+} exists in circulating cooling water operation systems. Fe_2O_3 formed after oxidation will deposit on pipes and equipment, which will easily cause corrosion under the scale. Therefore, copolymers must have good dispersible iron oxide properties. The influence of different concentrations of copolymers on dispersed iron oxide properties is shown in Figure 5.

As can be seen from Figure 5, the PAA and PESA concentrations have almost no effect of dispersing iron in this range. As the concentration of PASP increases, the light transmittance decreases, but the dispersion effect is weak. When the concentration of HEMA-AA-SAS is 5 mg/L, the light transmittance reaches about 50%. There is no yellowish-brown deposit in the test water sample, and the solution is yellow. It indicates that the copolymer has the best dispersing iron effect compared to the other three commercially available scale inhibitors. This is because the carboxyl group in the copolymer molecule forms a hydrophobic group with iron oxide, and the strong hydrophilic group of sulfonic group surrounds the hydrophobic group, to form a cluster structure, thereby achieving a better dispersing effect [21].

3.3.2. Effect of Copolymer Concentration on the Properties of Dispersed Silicon

Prepare 0.1% kaolin solution, add a certain concentration of Ca^{2+}, CO_3^{2-} solution and different concentrations of copolymer solution, mix thoroughly in a constant temperature

water bath at 50 °C for 5 h, and filter the supernatant after cooling to determine the turbidity of the solution at 420 nm; the greater the turbidity of the solution the better the dispersion of the copolymer silica effect.

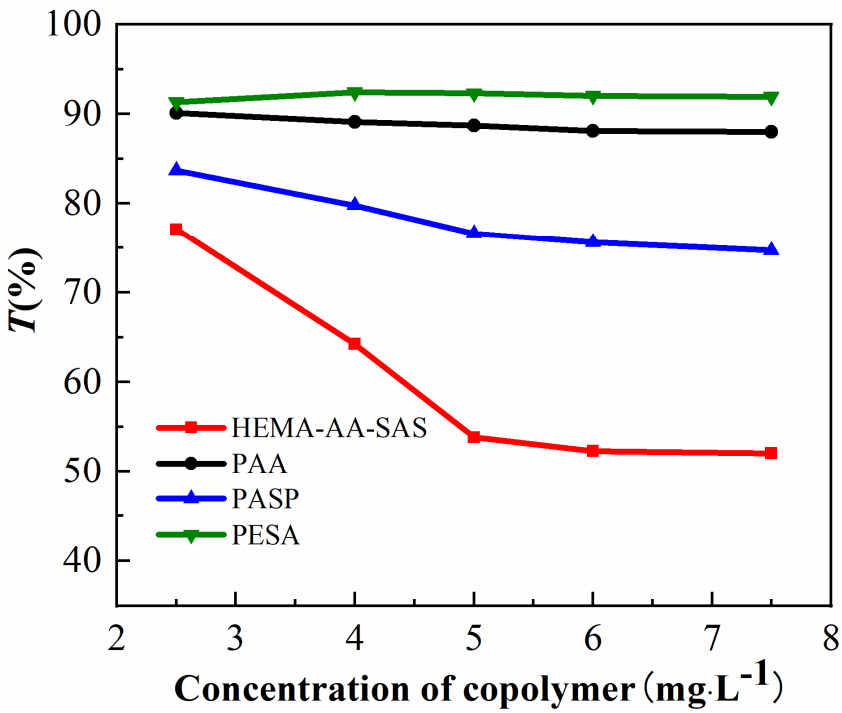

Figure 5. Influence of copolymer dosage on dispersibility iron performance.

The other reaction conditions were controlled constant, and the amount of scale inhibitor was changed to determine the dispersion effect of the four scale inhibitors on silicon at different concentrations; the results are shown in Figure 5.

Inorganic sediments are often produced in circulating water. The common scale compounds include silicate. When the content of silica in circulating the water is high, silicate scale is easily produced. Therefore, the copolymer is very important for the dispersion of silica properties. Figure 6 shows the effect on the properties of dispersed silicon at different dosages.

It can be seen that copolymer HEMA-AA-SAS has a better dispersing silicon effect. The concentration of the copolymer gradually increases in the test water sample, and its transmittance decreases. At this time, the turbidity of the water sample is larger, and the dispersing performance is stronger. The dispersing effect of PAA and PESA is worse. PASP has better dispersing ability for silicon than PAA and PESA, but the effect is general. At this time, the turbidity of the water sample is lower. It is basically clear, with obvious white sediments at the bottom.

3.4. Corrosion Inhibition of Copolymer HEMA-AA-SAS

3.4.1. Effect of Copolymer Addition on Corrosion Inhibition

The concentration of copolymer was 7.5 mg/L, and other conditions remained unchanged. The effect of copolymer dosage on corrosion inhibition is shown in Figure 7.

The corrosion inhibition rate increases and the corrosion rate decreases with the increase in the dosage of the copolymer scale inhibitor. This is due to the increase in carboxyl and sulfonic groups in the molecule and the formation of a compact film on the surface of carbon steel, which reduces the corrosion rate. The corrosion inhibition effect shows a continuous growth trend. When the dosage of the copolymer is low, the adsorption rate on the surface of carbon steel is low, and the corrosion inhibition effect is not obvious. When the concentration of copolymer is 7.5 mg/L, the corrosion inhibition rate is the best,

and the surface reaches a saturated state. When the concentration is 6 mg/L, the copolymer scale inhibitor reaches the dynamic equilibrium of adsorption and desorption on the surface of carbon steel; the corrosion inhibition rate increases slowly, and the copolymer molecules begin to agglomerate on the surface of carbon steel, which will cause the surface adsorption film not to be compact enough and the corrosion inhibition effect not to increase.

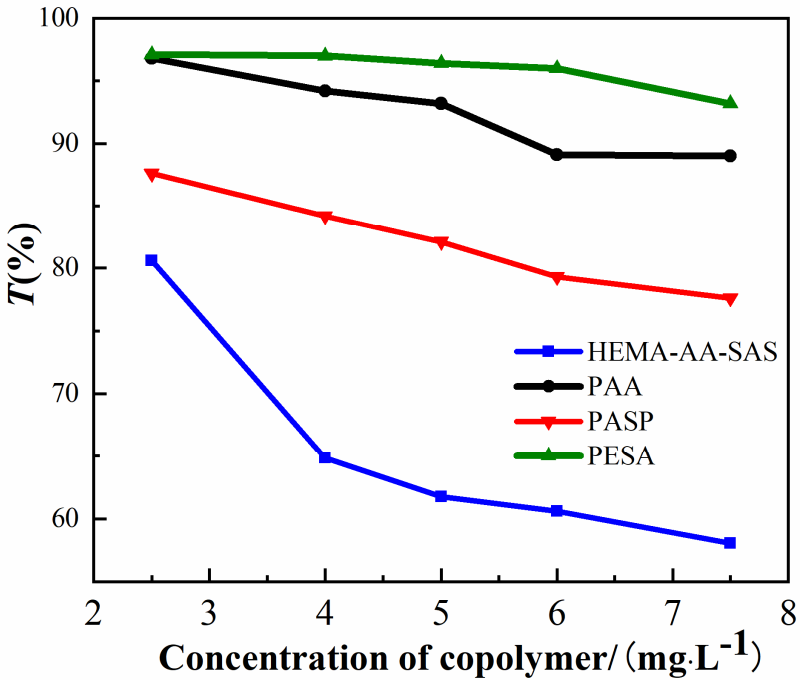

Figure 6. Influence of copolymer dosage on dispersibility silicon performance.

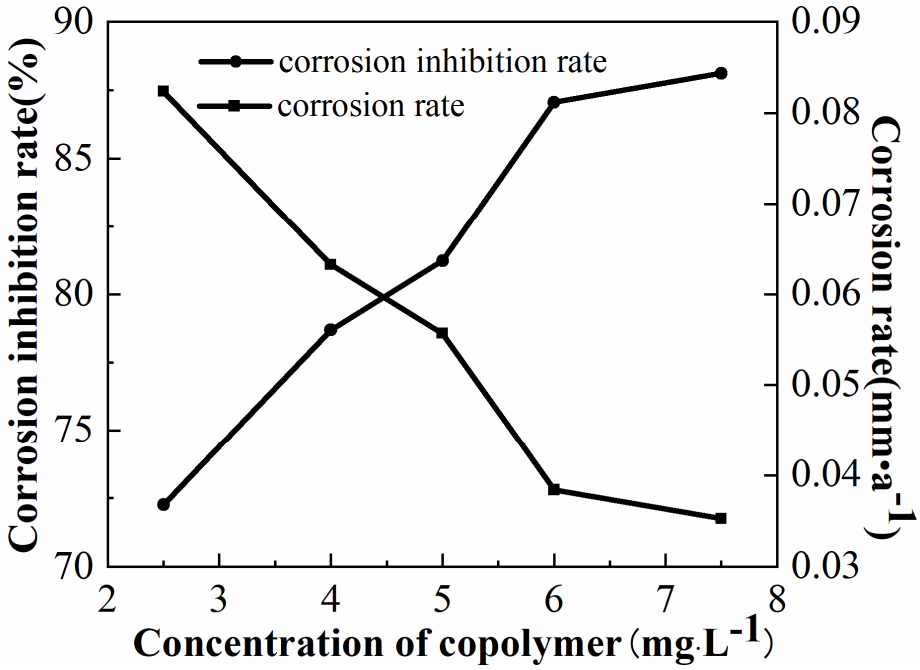

Figure 7. Influence of copolymer dosage on corrosion inhibition performance.

3.4.2. Effect of Water Sample Temperature on Corrosion Inhibition

The concentration of the copolymer was 7.5 mg/L, and other conditions remained unchanged. The effect of the reaction temperature on the corrosion inhibition of copolymers is shown in Figure 8.

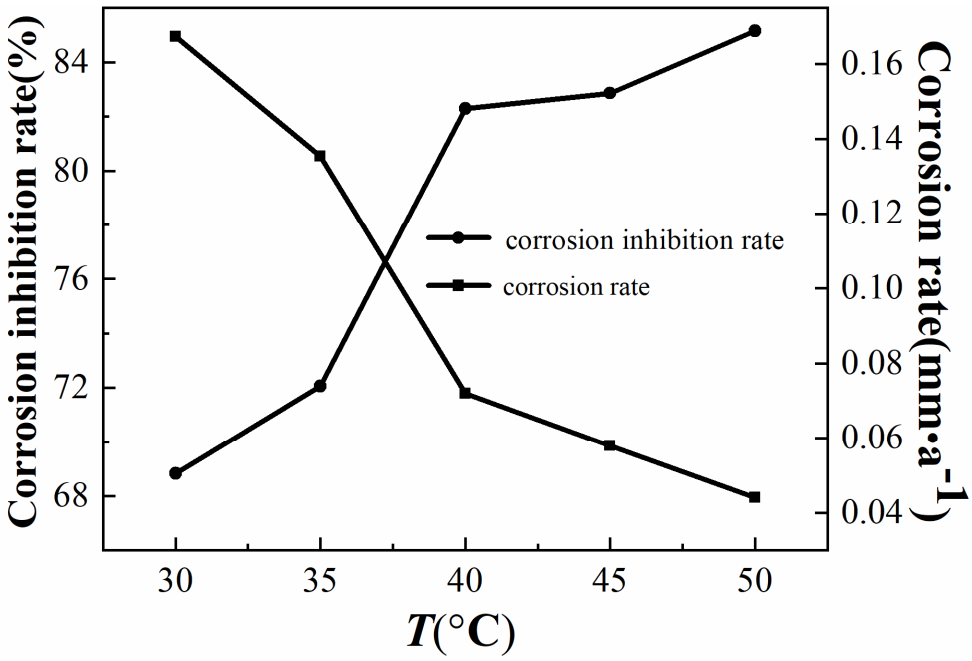

Figure 8. Influence of water sample temperature on corrosion inhibition.

With increasing temperature, the corrosion inhibition effect of copolymer scale inhibitor on carbon steel surface gradually increases. The adsorption of copolymer scale inhibitor on the carbon steel surface is an endothermic reaction. When the temperature rises to a certain level, the increasing trend of corrosion inhibition rate slows down because the adsorption behavior of copolymer on carbon steel surface decreases at a higher temperature. If the temperature continues to increase, desorption may occur, and the effective coverage of the adsorption film decreases [22]. When the temperature is relatively low, the equilibrium of adsorption and desorption can be shifted in the direction of adsorption by increasing the concentration.

3.4.3. Effect of pH of Water Sample on Corrosion Inhibition

The change in pH value in the water sample has a great influence on the corrosion inhibition effect of the copolymer because of the solubility of metal oxides will be affected in different pH environments [23]. The result of the pH value in the water sample on the corrosion inhibition effect of the copolymer is shown in Figure 9.

HEMA-AA-SAS is resistant to the hydrogen evolution thrust under acidic conditions, but the corrosion inhibition effect is better under alkaline conditions. This is due to the interaction of the reactive groups in the copolymer molecules [18]. When the test environment is acidic, the metal will undergo acidic corrosion [24], and the hydrogen escaped from acid corrosion will adsorb on the metal surface to destroy the adsorption film of corrosion inhibitor on the metal surface. The corrosion rate of the metal is accelerated. When the test environment is in neutral or alkaline conditions [25], it will promote the formation of the adsorption film on the metal surface, delay the corrosion rate of the metal, and improve the corrosion inhibition effect on metal.

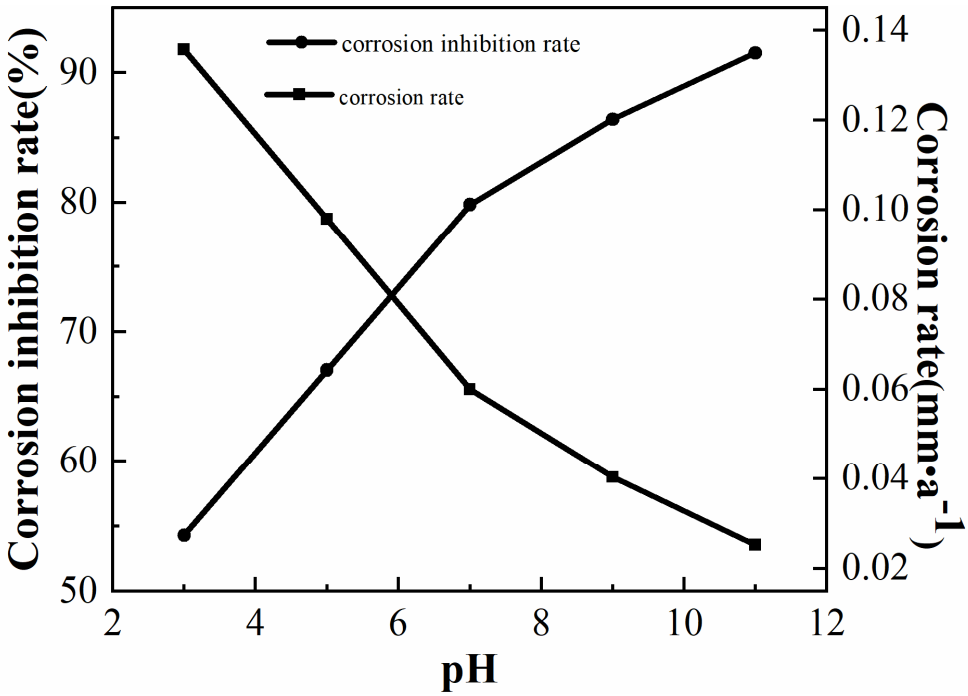

Figure 9. Influence of water sample pH on corrosion inhibition.

3.5. Analysis of Scale Inhibition Principle

The morphology and crystal structure of calcium carbonate were analyzed by SEM and XRD. Figure 10 shows the change in the crystal morphology of calcium carbonate before and after copolymer HEMA-AA-SAS treatment.

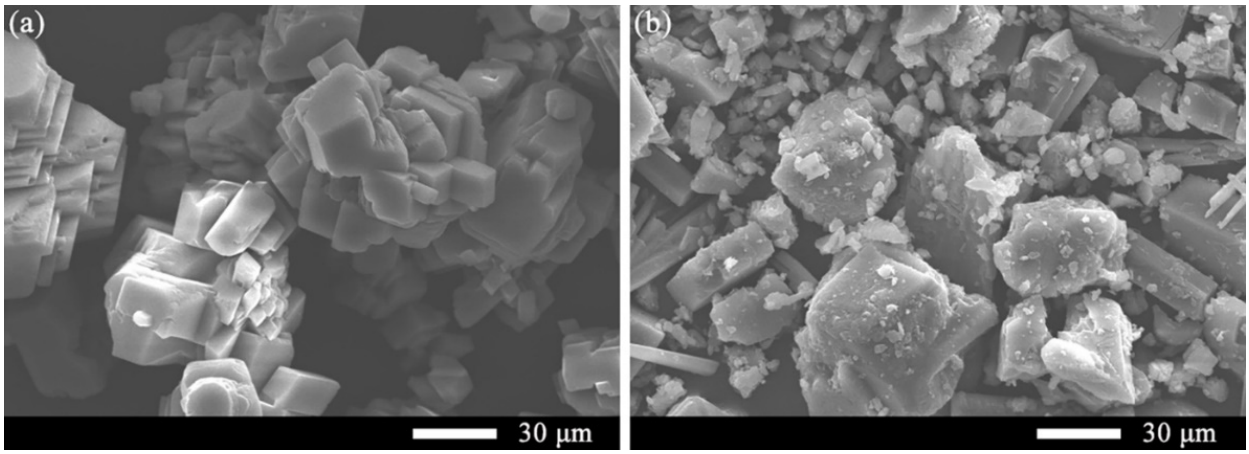

Figure 10. SEM of calcium carbonate crystals; (**a**) calcium carbonate crystal before adding copolymer; (**b**) calcium carbonate crystal after adding copolymer.

Figure 10a shows that when HEMA-AA-SAS is not added, the crystal has regular shape and structure, and it is easy to deposit scales on the pipes. Figure 10b shows the SEM image of calcium carbonate crystal after the addition of the copolymer. Comparing (a) with (b), it is found that the euhedral crystal morphology is obviously destroyed, and the shape is distorted [26]. This is because the active groups in the copolymer molecules adsorb on the active point of the crystals and inhibit the normal growth of crystals [27].

The crystal structure of calcium carbonate before and after copolymer treatment was analyzed using XRD.

Figure 11a shows the XRD when no copolymer scale inhibitor is added. The main diffraction peak is the most stable calcite in the thermodynamic state, such as 29° (104), 36° (110), 47.5° (018), 48.5° (118). Figure 11b shows the XRD after the addition of the copolymer scale inhibitor. Some of the calcite diffraction peaks have disappeared, with a strong vaterite diffraction peak at 27° (112) and an aragonite diffraction peak at 45° (221). The intensity of the crystal diffraction peaks is significantly lower after the copolymer is added, and the crystallinity of calcium carbonate decreases. It is indicated that after the copolymer HEMA-AA-SAS is added, the carboxyl group in the molecule complexed with Ca^{2+} and adsorbed on the surface growth point of calcium carbonate crystal [28] results in the decrease in crystallinity.

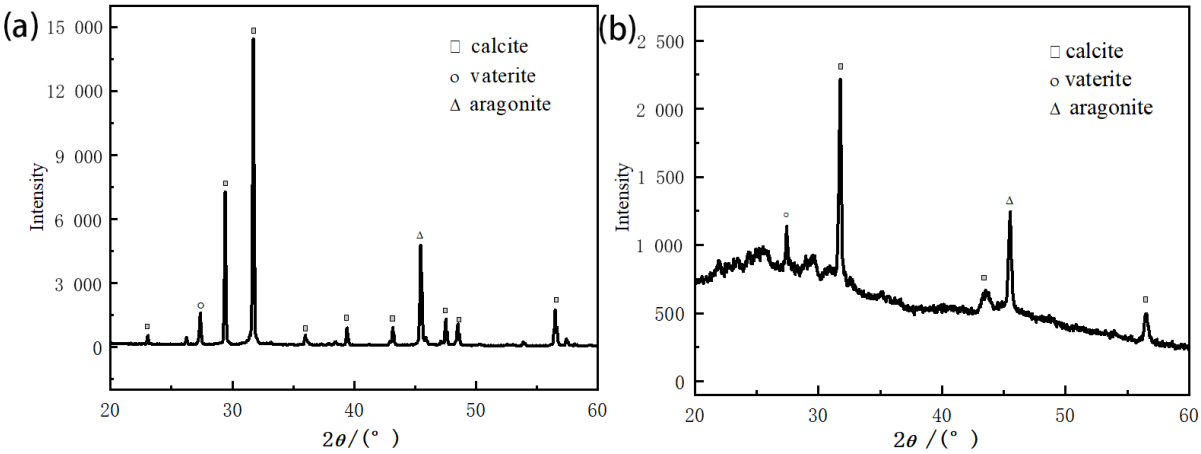

Figure 11. XRD of calcium carbonate crystals: (**a**) XRD of calcium carbonate without scale inhibitor and (**b**) XRD of Calcium Carbonate with Scale Inhibitor.

3.6. Analysis of Corrosion Inhibition Principle

3.6.1. Corrosion Kinetics

According to the Arrhenius equation:

$$\ln v = -\frac{E_a}{RT} + \ln A \tag{3}$$

where v is the corrosion rate, R is the standard thermodynamic constant, T is the thermodynamic temperature, E_a is the activation energy, and A is the pre-exponential factor.

According to Equation (3), it is known that there is a linear relationship between −lnV and 1/T. The activation energy can be calculated according to Equation (3), and the experimental results of corrosion activation energy are shown in Figure 12. The linear regression of the graph—lnν − 1/T is used to obtain the slope and intercept, R_2 = 0.9907 in the blank water sample and R_2 = 0.9806 in the water sample with a scale inhibitor. The linear correlation coefficients of both are close to 1, using the equation to calculate. The activation energies of the blank group and the added scale inhibitor are 25.17 KJ/mol and 60.87 KJ/mol, respectively. When the corrosion inhibitor (HEMA-AA-SAS) was added to the blank water sample, the activation energy of the reaction increased. The molecule of corrosion inhibitor adsorbs on the surface of the carbon steel sheet, which leads to the increase in the activation energy of the reaction, which in turn increases the difficulty of the corrosion reaction and weakens the corrosion effect of carbon steel. The results show that the copolymer has a good corrosion inhibition effect on carbon steel.

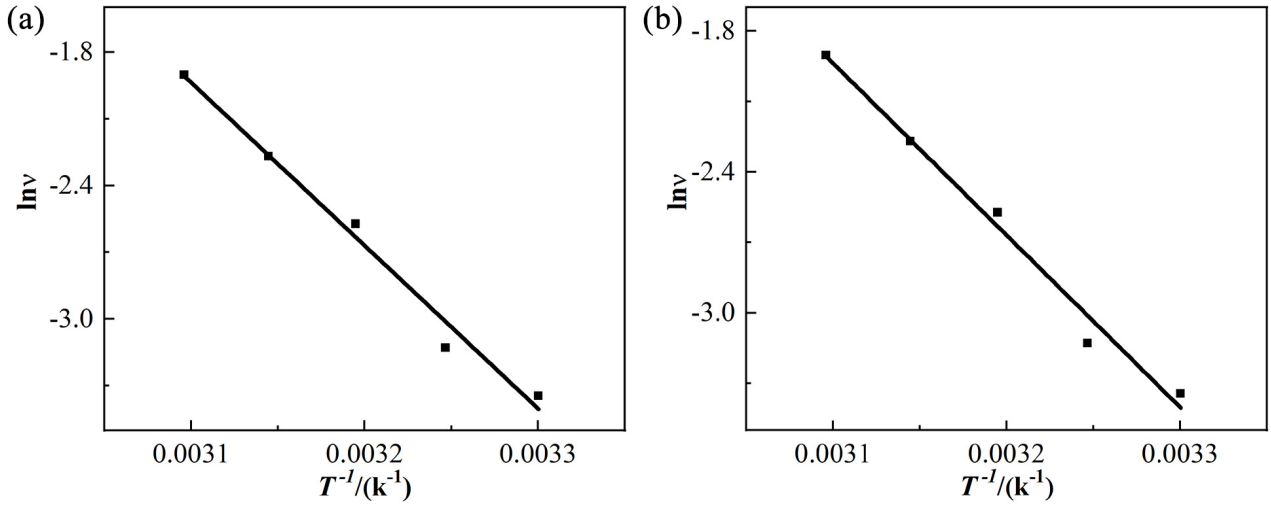

Figure 12. Comparison of corrosion activation energy; (**a**) ln ν and 1/T diagrams of blank water samples; (**b**) after adding copolymers.

3.6.2. Adsorption Thermodynamics

The effect of copolymer scale inhibitor on the surface of the carbon steel sheet is the geometric coverage effect. The corrosion inhibition rate is equal to coverage degree theta, and the adsorption conforms to the Langmuir adsorption isotherm:

$$\frac{\theta}{1-\theta} = K_{ads}C \tag{4}$$

or rewritten

$$\frac{C}{\theta} = C + \frac{1}{K_{ads}} \tag{5}$$

where C is the dosage concentration (mg/L), θ is the coverage rate, and K is the adsorption equilibrium constant.

As shown in Figure 13, the R_2 linear regression coefficient is 0.99861 close to 1. It shows that the adsorption of copolymer molecules on carbon steel hangings follows the Langmuir adsorption isotherm. The carboxyl sulfonate groups in the copolymer HEMA-AA-SAS formed a coordination bond with the D empty orbital of the iron atom [28], which formed a single molecule adsorption layer on the surface of carbon steel and effectively inhibited the corrosion reaction of carbon steel. The calculated adsorption equilibrium constant is 10.17 L/mg^{-1}.

The relationship between the standard free energy of adsorption and the equilibrium constant of adsorption:

$$K_{ads} = \frac{1}{55.5}\exp\left(-\frac{\Delta G_{ads}}{RT}\right) \tag{6}$$

The standard free energy of adsorption:

$$\Delta G_{ads} = -2.303RT\ln(55.5K_{ads}) \tag{7}$$

In the formula, 55.5 is the concentration of solvent water, mol/L; R is the gas constant, 8.314 J/mol; T is the thermodynamic temperature, K; K_{ads} is the adsorption equilibrium constant.

$|\Delta G_{ads}| \leq 20$ KJ/mol shows that the adsorption is mainly the physical adsorption of electrostatic interaction; $|\Delta G_{ads}| \geq 40$ KJ/mol shows that the adsorption is mainly the chemical adsorption of the covalent bond formed by charge sharing or transfer [14]; 20 KJ/mol $\leq |\Delta G_{ads}| \leq 40$ KJ/mol shows that the adsorption is a combination of two kinds of adsorption [29].

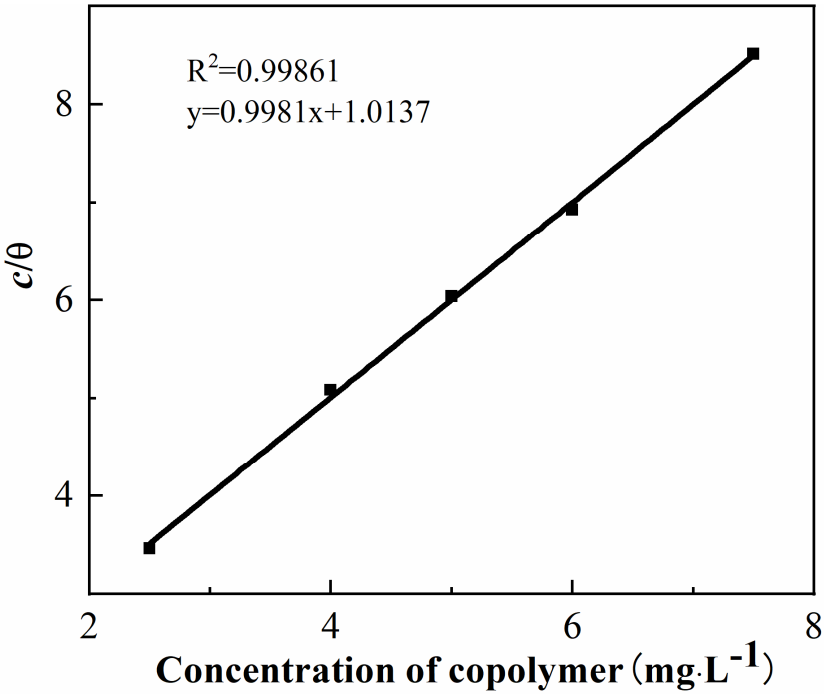

Figure 13. Adsorption isotherm.

The calculated standard free energy of adsorption ΔGads is −39.202 KJ/mol, and the result is negative, which indicates that the adsorption behavior of HEMA-AA-SAS on carbon steel coupons is spontaneous [30]. The absolute value of standard adsorption free energy is 39.202 KJ/mol. It shows that the copolymer is the result of the interaction of physical adsorption and chemical adsorption, and mainly based on chemical adsorption, rather than a single interaction [31,32].

4. Conclusions

(1) Under the same conditions, the scale inhibition effect and dispersion effect of low dose copolymer HEMA-AA-SAS are much higher than those of other commercial-scale inhibitors. At 6 mg/L, the scale inhibition effect is over 99%. This is because the copolymer molecule contains a large number of carboxyl groups, the main inhibition of calcium carbonate. In the determination of the properties of the copolymer for dispersed iron and silicon, the transmittance is less than 60% when the concentration of the copolymer is 7.5 mg/L. When the copolymer HEMA-AA-SAS concentration is 7.5 mg/L, the reaction temperature is 50 °C, under neutral or weak alkaline conditions, the best corrosion inhibition effect can reach more than 90%. The surface of the carbon steel hanging piece is smooth, and there is no obvious corrosion phenomenon.

(2) The results of SEM and XRD analysis show that the crystal structure of calcium carbonate is distorted after adding the copolymer. Before adding the copolymer, the crystals of calcium carbonate are mainly calcite. Under the action of the copolymer, the structure is more irregular, with additional aragonite and vaterite, and the crystals cannot grow euhedrally.

(3) The calculation of corrosion kinetics and adsorption thermodynamics showed that the copolymer had good corrosion inhibition performance. The copolymer formed a dense film spontaneously on the metal surface by chemical adsorption. Compared with the blank water sample, the activation energy of corrosion increased after adding copolymer HEMA-AA-SAS, and the barrier needed to overcome the corrosion reaction increased, which slowed down the corrosion rate and prevented the corrosion on the surface of carbon steel specimens.

Author Contributions: R.Y.: conceptualization (equal), writing—review and editing. H.L.: formal analysis, conceptualization (equal), writing—original draft, investigation (equal). Z.T.: validation investigation (equal), conceptualization (equal). All authors have read and agreed to the published version of the manuscript.

Funding: This research received no external funding.

Data Availability Statement: Data sharing is not applicable to this article as no new data were created or analyzed in this study.

Acknowledgments: We acknowledge support from the Industrial Key Scientific and Technological Project, Shaanxi, China (No. 2015GY101) and thank the Center Laboratory of the Water Treatment of Xi'an Polytechnic University, China.

Conflicts of Interest: The authors declare no competing financial interest.

References

1. Li, H.; Ren, D.; Zhuang, M.; Wang, Z.; Zhang, X.; Zhang, S.; Chen, W. Synthesis and property study of a polyether TERCOPOLYMER scale inhibitor with carboxyl and sulfonic acid groups. *J. Appl. Polym. Sci.* **2021**, *139*, 51505. [CrossRef]
2. Yu, L.; Bao, J.; Wang, G.; Lu, W.; Chen, W. Structure and properties of gel-spun ultra-high molecular weight polyethylene fibers obtained from industrial production line. *J. Appl. Polym. Sci.* **2021**, *138*, 51317. [CrossRef]
3. Sanatgar, R.H.; Cayla, A.; Campagne, C.; Nierstrasz, V. Morphological and electrical characterization of conductive polylactic acid based nanocomposite before and after FDM 3D printing. *J. Appl. Polym. Sci.* **2018**, *136*, 47040. [CrossRef]
4. Wang, C.; Shen, T.; Li, S.; Wang, X. Investigation of influence of low phosphorous co-polymer antiscalant on calcium sulfate dihydrate crystal morphologies. *Desalination* **2014**, *348*, 89–93. [CrossRef]
5. Liu, F.; Lu, X.; Yang, W.; Lu, J.; Zhong, H.; Chang, X.; Zhao, C. Optimizations of inhibitors compounding and applied conditions in simulated circulating cooling water system. *Desalination* **2013**, *313*, 18–27. [CrossRef]
6. Ruelo, M.T.G.; Tijing, L.D.; Amarjargal, A.; Park, C.H.; Kim, H.J.; Pant, H.R.; Lee, D.H.; Kim, C.S. Assessing the effect of catalytic materials on the scaling of Carbon Steel. *Desalination* **2013**, *313*, 189–198. [CrossRef]
7. Karar, A.; Henni, A.; Namoune, F.; Rosei, F. Inhibition of nucleation and crystal growth of calcium carbonate in hard waters using paronychia arabica in an arid desert region. *Water Environ. J.* **2020**, *34*, 979–987. [CrossRef]
8. Abdel-Aal, E.A.; Abdel-Ghafar, H.M.; El Anadouli, B.E. New findings about nucleation and crystal growth of reverse osmosis desalination scales with and without inhibitor. *Cryst. Growth Des.* **2015**, *15*, 5133–5137. [CrossRef]
9. Purgstaller, B.; Goetschl, K.E.; Mavromatis, V.; Dietzel, M. Solubility investigations in the amorphous calcium magnesium carbonate system. *CrystEngComm* **2019**, *21*, 155–164. [CrossRef]
10. Roomi, Y.A.; Hussein, K.F.; Riazi, M.R. Inhibition efficiencies of synthesized anhydride based polymers as scale control additives in petroleum production. *J. Pet. Sci. Eng.* **2012**, *81*, 151–160. [CrossRef]
11. Usmany, Y.; Putranto, W.A.; Bayuseno, A.P.; Muryanto, S. Crystallization of calcium carbonate ($CaCO_3$) in a flowing system: Influence of Cu^{2+} additives on induction time and crystalline phase transformation. In *AIP Conference Proceedings*; AIP Publishing LLC: Melville, NY, USA, 2016. [CrossRef]
12. Asaeda, T.; Senavirathna, M.D.H.J.; Kaneko, Y.; Rashid, M.H. Effect of calcium and magnesium on the growth and calcite encrustation of Chara fibrosa. *Aquat. Bot.* **2014**, *113*, 100–106. [CrossRef]
13. Mohammad, S. Corrosion Protection and Computational Simulation of Functional Epoxy Coating on 2024-T3 Aluminum Alloy. Ph.D. Thesis, University of Science and Technology of China, Hefei, China, 2021. Available online: https://lib-vpn.xpu.edu.cn:443/rwt/CNKI/https/NNYHGLUDN3WXTLUPMW4A/KCMS/detail/detail.aspx?dbname=CDFDLAST2021&filename=1021040978.nh (accessed on 2 February 2021).
14. Liu, G.; Xue, M.; Liu, Q.; Yang, H.; Yang, J.; Zhou, Y. Maleic anhydride–allylpolyethoxy carboxylate copolymer as an effective and environmentally benign inhibitor for calcium carbonate in industrial cooling systems. *RSC Adv.* **2017**, *7*, 24723–24729. [CrossRef]
15. Touir, R.; Cenoui, M.; El Bakri, M.; Touhami, M.E. Sodium gluconate as corrosion and scale inhibitor of ordinary steel in simulated cooling water. *Corros. Sci.* **2008**, *50*, 1530–1537. [CrossRef]
16. Woudma, S.K. Study on Corrosion Inhibition Mechanism of Copper and Copper Alloy by Environmentally Friendly Corrosion Inhibitor in Salt Solutions. Ph.D. Thesis, University of Science and Technology Beijing, Bejing, China, 2020. Available online: https://lib-vpn.xpu.edu.cn:443/rwt/CNKI/https/NNYHGLUDN3WXTLUPMW4A/KCMS/detail/detail.aspx?dbname=CDFDLAST2021&filename=1020109100.nh (accessed on 13 July 2020).
17. Naka, K. Effect of dendrimers on the crystallization of calcium carbonate in aqueous solution. *Top. Curr. Chem.* **2003**, *228*, 141–158. [CrossRef] [PubMed]
18. Gu, X.; Qiu, F.; Zhou, X.; Qi, J.; Zhou, Y.; Yang, D.; Guo, Q.; Guo, X. Preparation and application of polymers as inhibitors for calcium carbonate and calcium phosphate scales. *Int. J. Polym. Mater. Polym. Biomater.* **2013**, *62*, 323–329. [CrossRef]
19. Change, F.; Yuming, Z.; Guangqing, L.; Jingyi, H.; Wei, S.; Wendao, W. Inhibition of $Ca_3(PO_4)_2$, $CaCO_3$, and $CaSO_4$ precipitation for industrial recycling water. *Ind. Eng. Chem. Res.* **2011**, *50*, 10393–10399. [CrossRef]

20. Amjad, Z.; Koutsoukos, P.G. Evaluation of maleic acid based polymers as scale inhibitors and dispersants for Industrial Water Applications. *Desalination* **2014**, *335*, 55–63. [CrossRef]
21. Huang, H.; Yao, Q.; Jiao, Q.; Liu, B.; Chen, H. Polyepoxysuccinic acid with hyper-branched structure as an environmentally friendly scale inhibitor and its scale inhibition mechanism. *J. Saudi Chem. Soc.* **2019**, *23*, 61–74. [CrossRef]
22. Han, P.; Chen, C.; Li, W.; Yu, H.; Xu, Y.; Ma, L.; Zheng, Y. Synergistic effect of mixing cationic and nonionic surfactants on corrosion inhibition of mild steel in HCL: Experimental and theoretical investigations. *J. Colloid Interface Sci.* **2018**, *516*, 398–406. [CrossRef] [PubMed]
23. Finšgar, M. 2-Mercaptobenzimidazole as a copper corrosion inhibitor: Part I long-term immersion, 3D-profilometry, and electrochemistry. *Corros. Sci.* **2013**, *72*, 82–89. [CrossRef]
24. Wei, B.M. *Theory and Application of Metal Corrosion*; Chemical Industry Press: Beijing, China, 2004.
25. Lalitha, A.; Ramesh, S.; Rajeswari, S. Surface protection of copper in acid medium by azoles and surfactants. *Electrochim. Acta* **2005**, *51*, 47–55. [CrossRef]
26. Al-Hamzah, A.A.; East, C.P.; Doherty, W.O.; Fellows, C.M. Inhibition of homogenous formation of calcium carbonate by poly (acrylic acid). the effect of molar mass and end-group functionality. *Desalination* **2014**, *338*, 93–105. [CrossRef]
27. Chaussemier, M.; Pourmohtasham, E.; Gelus, D.; Pécoul, N.; Perrot, H.; Lédion, J.; Cheap-Charpentier, H.; Horner, O. State of art of natural inhibitors of calcium carbonate scaling. A review article. *Desalination* **2015**, *356*, 47–55. [CrossRef]
28. Simonović, A.T.; Petrović, M.B.; Radovanović, M.B.; Milić, S.M.; Antonijević, M.M. Inhibition of copper corrosion in acidic sulphate media by eco-friendly amino acid compound. *Chem. Pap.* **2014**, *68*, 362–371. [CrossRef]
29. Tebbji, K.; Faska, N.; Tounsi, A.; Oudda, H.; Benkaddour, M.; Hammouti, B. The effect of some lactones as inhibitors for the corrosion of mild steel in 1M hydrochloric acid. *Mater. Chem. Phys.* **2007**, *106*, 260–267. [CrossRef]
30. Outirite, M.; Lagrenée, M.; Lebrini, M.; Traisnel, M.; Jama, C.; Vezin, H.; Bentiss, F. AC impedance, X-ray photoelectron spectroscopy and density functional theory studies of 3,5-bis(n-pyridyl)-1,2,4-oxadiazoles as efficient corrosion inhibitors for carbon steel surface in hydrochloric acid solution. *Electrochim. Acta.* **2010**, *55*, 1670–1681. [CrossRef]
31. Hu, S.Q.; Hu, J.C.; Gao, Y.J.; Jia, X.L.; Guo, W.Y. Corrosion inhibition and adsorption of laury-l imidazolines for Q235 steel. *CIESC J.* **2011**, *62*, 147–155. Available online: https://hgxb.cip.com.cn/EN/Y2011/V62/I1/147 (accessed on 15 January 2011).
32. Yurt, A.; Ulutas, S.; Dal, H. Electrochemical and theoretical investigation on the corrosion of aluminium in acidic solution containing some Schiff bases. *Appl. Surf. Sci.* **2006**, *253*, 919–925. [CrossRef]